



Contents lists available at ScienceDirect

## Applied Mathematical Modelling

journal homepage: [www.elsevier.com/locate/apm](http://www.elsevier.com/locate/apm)

## On non-Newtonian lubrication with the upper convected Maxwell model

Xin Kai Li<sup>a,\*</sup>, Yingshe Luo<sup>b</sup>, Yuanwei Qi<sup>c</sup>, Rong Zhang<sup>d</sup><sup>a</sup> Faculty of Technology, De Montfort University, Leicester, LE1 9BH, UK<sup>b</sup> IRMME, The Centre South University of Forestry and Technology, Changsha, China<sup>c</sup> Department of Mathematics, University of Central Florida, Orlando, FL 32816-1364, USA<sup>d</sup> Department of Computing Sciences, Southern Yangtze University, Jiangsu, China

## ARTICLE INFO

## Article history:

Received 21 August 2008

Received in revised form 27 September 2010

Accepted 12 November 2010

Available online xxx

## Keywords:

Viscoelasticity

Non-Newtonian lubricant

Perturbation method

Thin film

Maxwell model

## ABSTRACT

A long-standing theoretical and practical problem, whether the viscoelasticity can have a measurable and beneficial effect on lubrication performance characteristics, is readdressed in this paper. The upper convected Maxwell model is chosen to study the influence of viscoelasticity on lubricant thin film flows. By employing characteristic lubricant relaxation times in an order of magnitude analysis, a perturbation method is developed for analysing the flow of a Maxwell lubricant between two narrow surfaces. The effect of viscoelasticity on the lubricant velocity and pressure is examined, and the influence of minimum film thickness on lubrication characteristics is investigated. An order of magnitude analysis reveals that the pressure distribution is significantly affected by the presence of fluid viscoelasticity when the minimum film thickness is sufficiently small. This mechanism suggests that viscoelasticity does indeed enhance the lubricant pressure field and produce a beneficial effect on lubrication performance, which is consistent with some experimental observations.

© 2010 Elsevier Inc. All rights reserved.

## 1. Introduction

A fascinating and largely-unresolved problem in tribology concerns the effect of viscoelasticity on lubrication characteristics in thin film flows. The problem has been tackled since the mid-1950s with the appearance of the so called multigrade oils [1–5], and has recently taken on added significance with the lower-viscosity lubricants for improved energy efficiency. Any factor influencing load capacity and wear on lubricating systems is clearly of renewed importance, in particular, for the protection of the green environment. There are good theoretical and practical reasons to reopen the general question of viscoelastic effects on lubrication characteristics [6,7].

Since the mid 1950s, the addition of polymers to mineral oils has become a well established practice. These additives cause the resulting lubricants to become non-Newtonian and viscoelastic [1,3,8]. Even in the simplest flow situation, it is necessary to consider more than the usual shear-stress component, and the mechanical behaviour of these lubricants is potentially far more complicated than that of mineral oil based lubricants, which may be regarded as Newtonian fluids. It is known that polymeric-additive-containing lubricants possess a characteristic relaxation time,  $\lambda$ , which is the ratio of the viscosity to the elastic modulus. For lubricating oils the fluid relaxation times might be expected to vary from  $10^{-3}$  to  $10^{-6}$  s [8,9]. If a lubrication process time is of the same order, one could expect strong time-dependent effects. The Deborah number  $De = \lambda/T$  is usually to be used to measure such time dependence, where  $T$  is a characteristic time of the flow process under consideration [2,9].

\* Corresponding author. Tel.: +44 (0) 1162078695; fax: +44 (0) 1162541891.

E-mail address: [xkl@dmu.ac.uk](mailto:xkl@dmu.ac.uk) (X.K. Li).

Attempts to interpret this time-dependent effect on the basis of a shear dependent viscosity alone, or on the different heat transfer characteristics of polymeric lubricants, have proved largely unproductive, and the viscoelastic behaviour of the lubricants has been proposed as the most likely cause for the improvements in performance [5,8,10]. Despite popular belief and some experimental evidences with real lubricants [8], it appears that unequal normal stresses and memory effects may be relatively insignificant in the lubricating systems [5]. As a consequence, one might superficially expect that, at high shear rates encountered in well-designed optimally loaded bearings, the behaviour of multi-grade oils may not be greatly different from that of the low viscosity base stock used to formulate oils [3]. In a recent study, however, values of the minimum film thickness obtained from direct measurements in an instrumented front-main bearing of an operating engine were found to correlate not with the high temperature, high shear rate viscosity alone, but with a combination of the high temperature, high shear rate viscosity and relaxation time-viscoelasticity [7,8]. The relaxation times were calculated based on primary normal stress measurements made using a Lodge stress-meter by Cameron [7]. Even though typical fluid relaxation times are only of the order of microseconds, viscoelasticity can have a measurable and beneficial effect on lubrication characteristics [7], and is expected to significantly affect the minimum film thickness and the coefficients of friction in the thin-film flows [6,7,11].

There is some controversy as to whether viscoelastic behaviour as manifested through normal stress effects can have any effect at all in lubrication, over and above that which arises as a result of the shear dependence of the viscosity [11,12]. It now seems clear that polymeric oils are in fact better lubricants than non-polymeric oils, at least in the application of lubricating systems [7,8]. Specifically, they appear to reduce friction and wear when compared with either their base oils or mineral oils of comparable low-shear viscosity [11]. To date, attempts to predict this improvement in performance by invoking non-Newtonian behaviour have been singularly unsuccessful. It is unlikely that one could have known *a priori* whether viscoelasticity would give rise to any beneficial or adverse side effects, although the fact that one of nature's lubricants, synovial fluid, is viscoelastic was perhaps a useful pointer [7,8,10]. Over the past decades, numerous theoretical and experimental studies have been undertaken to determine whether polymer-improved liquids are more efficient than their Newtonian counterparts, even after the improved viscosity-temperature response has been accommodated [8]. It is fair to say that the situation is inconclusive and somewhat confused. At best, there have been small improvements presented in [8], and further extended in [7,13]; at worst, any effects have been within the experimental errors (see [6,12,14,15]).

Early studies on thin film flows have used lubrication theory to derive a coupled system of equations governing the spatial and temporal evolution of the film thickness, see [3,5,10]. The majority of these works have concentrated on Newtonian fluids, and sought to elucidate the fundamental mechanism of thin film flow in various applications. Reviews covering these works can be found in [5,10,16]. Recently, significant attention has been devoted to non-Newtonian fluids in thin film flows, since in many practical applications thin films generally exhibit non-Newtonian behaviour. We refer to the works in [10,16–19]. The aim of this article is to extend our previous results [20,21] and investigate how the presence of viscoelasticity modifies the lubricant characteristics in the thin film flows.

In this paper, the lubricant behaviour is modelled by an upper convected Maxwell (UCM) constitutive equation, which is the simplest viscoelastic model having a constant viscosity and a constant relaxation time. By employing characteristic relaxation time in an order of magnitude analysis, a perturbation method is developed to analyse the flow of Maxwell viscoelastic lubricants between two narrow surfaces and determine whether the viscoelastic properties have any effects on lubrication characteristics compared with their Newtonian counterparts.

In the following section, we present the basic UCM equations with relevant scalings. In Section 3, we outline the perturbation method and provide asymptotic solutions for thin film flows. A detail of derivation of these solutions is supplied in Appendix A. In Section 4, we present a discussion of numerical simulations with various film surfaces. Finally, we summarize the conclusions and remarks in Section 5.

## 2. Mathematical model

One of the simplest viscoelastic fluid models available is the upper convected Maxwell model incorporating a constant viscosity and a relaxation time. In this study, we restrict our attention to the UCM constitutive model characterized by a small relaxation time. Following [2], the equations of motion and continuity for unsteady incompressible flow are, respectively,

$$\rho \left( \frac{\partial \mathbf{v}}{\partial t} + \mathbf{v} \cdot \nabla \mathbf{v} \right) = \mathbf{b} - \nabla p - \nabla \cdot \boldsymbol{\tau} \quad (1)$$

and

$$\nabla \cdot \mathbf{v} = 0, \quad (2)$$

where  $\mathbf{v} = (u, v)$  is the velocity vector,  $p$  is the isotropic pressure,  $\boldsymbol{\tau}$  is the extra-stress tensor,  $\mathbf{b}$  is the body force and  $\rho$  is the density of the fluid. The extra-stress tensor is related to the rate-of-strain tensor by a constitutive equation. The UCM model is given by

$$\lambda \overset{\nabla}{\boldsymbol{\tau}} + \boldsymbol{\tau} = -2\eta \mathbf{d}, \quad (3)$$

where  $\lambda$  is characteristic relaxation time of the fluid, and  $\eta$  is the lubricant viscosity, and

$$\mathbf{d} = \frac{1}{2} (\nabla \mathbf{v} + (\nabla \mathbf{v})^T) \quad (4)$$

is the rate of deformation tensor, and  $\overset{\nabla}{\tau}$  is the upper convected derivative defined as

$$\overset{\nabla}{\tau} = \frac{\partial \tau}{\partial t} + \mathbf{v} \cdot \nabla \tau - (\nabla \mathbf{v}) \cdot \tau - \tau \cdot (\nabla \mathbf{v})^T. \quad (5)$$

In general,  $\lambda$  and  $\eta$  are functions of the local shear rate, pressure and temperature, see [14,15,22]. For simplicity, they are taken to be constant in this paper.

A typical two-dimensional thin film flow problem is illustrated in Fig. 1, where the space between two surfaces in relative motion is filled with a non-Newtonian fluid. In this problem, we assume that the characteristic length  $L$  in the  $x$ -direction is much greater than the characteristic length  $H_0$  in the  $y$ -direction. Under the experimentally possible processing conditions, the fluid may be assumed to be steady incompressible and inertialess, and the gravitation effects are negligible ( $\mathbf{b} = \mathbf{0}$ ). The continuity and momentum equations for steady flow can be rewritten in component form as

$$\frac{\partial u}{\partial x} + \frac{\partial v}{\partial y} = 0, \quad (6)$$

$$\frac{\partial \tau_{xx}}{\partial x} + \frac{\partial \tau_{xy}}{\partial y} + \frac{\partial p}{\partial x} = 0, \quad (7)$$

$$\frac{\partial \tau_{xy}}{\partial x} + \frac{\partial \tau_{yy}}{\partial y} + \frac{\partial p}{\partial y} = 0. \quad (8)$$

The constitutive Eq. (3) in component form becomes

$$\tau_{xx} + \lambda \left( u \frac{\partial \tau_{xx}}{\partial x} + v \frac{\partial \tau_{xx}}{\partial y} - 2 \frac{\partial u}{\partial y} \tau_{xy} - 2 \frac{\partial u}{\partial x} \tau_{xx} \right) = -2\eta \frac{\partial u}{\partial x}, \quad (9)$$

$$\tau_{xy} + \lambda \left( u \frac{\partial \tau_{xy}}{\partial x} + v \frac{\partial \tau_{xy}}{\partial y} - \frac{\partial u}{\partial y} \tau_{yy} - \frac{\partial v}{\partial x} \tau_{xx} \right) = -\eta \left( \frac{\partial u}{\partial y} + \frac{\partial v}{\partial x} \right), \quad (10)$$

$$\tau_{yy} + \lambda \left( u \frac{\partial \tau_{yy}}{\partial x} + v \frac{\partial \tau_{yy}}{\partial y} - 2 \frac{\partial v}{\partial y} \tau_{yy} - 2 \frac{\partial v}{\partial x} \tau_{xy} \right) = -2\eta \frac{\partial v}{\partial y}. \quad (11)$$

The boundary conditions for flow confined between two rigid surfaces, the lower of which is sliding in  $x$  direction at velocity  $U$ , see Fig. 1, are as follows:

$$u = U, \quad v = 0, \quad \text{when } y = 0, \quad (12)$$

$$u = 0, \quad v = 0, \quad \text{when } y = H(x). \quad (13)$$

Here, Eqs. (12) and (13) express no-slip boundary condition at both surfaces.

The stress boundary conditions are more complicated. Physically, one boundary condition states that (for the case of a liquid–gas interface) there is no shear stress at tangential to the interface. The other states that the stress normal to the interface must be balanced by a stress acting normal to the surface arising from surface tension, and described by the

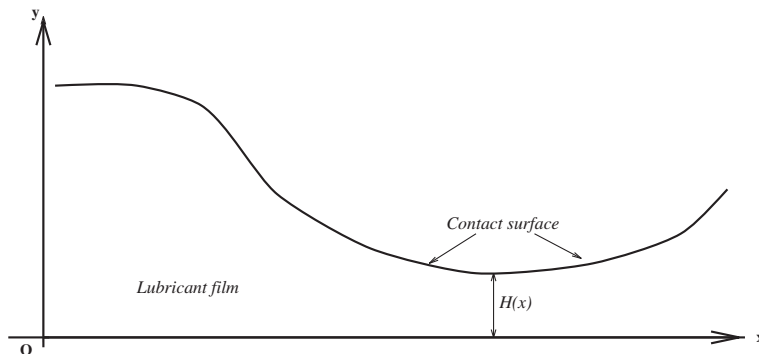


Fig. 1. Geometry for a lubricant thin film flow.

Young–Laplace equation (see Chapter 2 in [23]). In this paper, we assume that the state of stresses at some point on the inlet or on the outlet boundaries is determined by the stress tensor within the liquid phase, and assume that the external fluid (taken to be a gas, here) is stress free. The stress boundary conditions on the normal stress are given by the Young–Laplace equation as follows:

$$p - \eta \frac{\partial v}{\partial y} = 0, \quad \text{when } x = 0 \quad \text{and} \quad x = L. \quad (14)$$

Further discussion of the boundary conditions can be found in [3,5,10,16,23,24].

The governing equations can be expressed in dimensionless forms by defining the following dimensionless quantities

$$\begin{aligned} x^* &= \frac{x}{L}, \quad y^* = \frac{y}{H_0}, \quad u^* = \frac{u}{U}, \quad v^* = \frac{v}{UH_0/L}, \\ \tau_{xx}^* &= \frac{\tau_{xx}}{\eta UL/H_0^2}, \quad \tau_{xy}^* = \frac{\tau_{xy}}{\eta U/H_0}, \quad \tau_{yy}^* = \frac{\tau_{yy}}{\eta U/L}, \\ p^* &= \frac{p}{\eta UL/H_0^2}, \quad De = \frac{\lambda U}{L}, \quad \epsilon = \left(\frac{H_0}{L}\right)^2, \quad h(x) = \frac{H(x)}{H_0}. \end{aligned} \quad (15)$$

The concept of the Deborah number,  $De$ , highlights that it is not only the material's relaxation time,  $\lambda$ , which determines material behaviour, but also the time-scale of the deformation process. At high Deborah number, the fluid responds like a solid, while, at low Deborah number the fluid responds like a liquid. The Deborah number is less than one for the polymeric lubricants. Clearly, the Deborah number is zero for a Newtonian fluid and infinite for a Hookean elastic solid (see [2,9]).

Substituting the dimensionless variables (15) in equations (6)–(11), and dropping the asterisks, we obtain the dimensionless governing equations

$$\frac{\partial u}{\partial x} + \frac{\partial v}{\partial y} = 0, \quad (16)$$

$$\frac{\partial \tau_{xx}}{\partial x} + \frac{\partial \tau_{xy}}{\partial y} + \frac{\partial p}{\partial x} = 0, \quad (17)$$

$$\epsilon \left( \frac{\partial \tau_{xy}}{\partial x} + \frac{\partial \tau_{yy}}{\partial y} \right) + \frac{\partial p}{\partial y} = 0, \quad (18)$$

$$\tau_{xx} + De \left( u \frac{\partial \tau_{xx}}{\partial x} + v \frac{\partial \tau_{xx}}{\partial y} - 2 \frac{\partial u}{\partial y} \tau_{xy} - 2 \frac{\partial u}{\partial x} \tau_{xy} \right) = -2\epsilon \frac{\partial u}{\partial x}, \quad (19)$$

$$\tau_{xy} + De \left( u \frac{\partial \tau_{xy}}{\partial x} + v \frac{\partial \tau_{xy}}{\partial y} - \frac{\partial u}{\partial y} \tau_{yy} - \frac{\partial v}{\partial x} \tau_{xx} \right) = - \left( \frac{\partial u}{\partial y} + \epsilon \frac{\partial v}{\partial y} \right), \quad (20)$$

$$\tau_{yy} + De \left( u \frac{\partial \tau_{yy}}{\partial x} + v \frac{\partial \tau_{yy}}{\partial y} - 2 \frac{\partial v}{\partial y} \tau_{yy} - 2 \frac{\partial v}{\partial x} \tau_{xy} \right) = -2 \frac{\partial v}{\partial y} \quad (21)$$

and the boundary conditions become

$$u = 1, \quad v = 0, \quad \text{when } y = 0, \quad (22)$$

$$u = 0, \quad v = 0, \quad \text{when } y = h(x), \quad (23)$$

$$p - \epsilon \frac{\partial v}{\partial y} = 0, \quad \text{when } x = 0, \quad \text{and} \quad x = 1. \quad (24)$$

Finally, it should be mentioned that in most of cases, bubbles may appear in the convergent–divergent region, as shown in Fig. 1, due to the pressure falling below the saturation pressure yielding a cavitation region. Since the governing equations are no longer valid in such a region, a cavitation model developed either by the form of variational inequality [25] or by introducing an additional unknown for the fluid saturation pressure [15,22] has to be considered. For the technical details of the implementation of the cavitation models, the reader is referred to Refs. [5,10,15,22,25,26].

### 3. Perturbation analysis

In this section we use a regular perturbation expansion to analyse Eqs. (16)–(21) subject to the boundary conditions (22)–(24). Specifically, we assume an asymptotic solution in the form of a double perturbation expansion as power series of  $De$  and  $\epsilon$ :

$$\begin{aligned}
u &= u^{[\ell]} + Deu^{[D]} + \epsilon u^{[\epsilon]} + O(De^2) + O(\epsilon^2), \\
v &= v^{[\ell]} + Dev^{[D]} + \epsilon v^{[\epsilon]} + O(De^2) + O(\epsilon^2), \\
\tau_{xx} &= \tau_{xx}^{[\ell]} + De\tau_{xx}^{[D]} + \epsilon\tau_{xx}^{[\epsilon]} + O(De^2) + O(\epsilon^2), \\
\tau_{yy} &= \tau_{yy}^{[\ell]} + De\tau_{yy}^{[D]} + \epsilon\tau_{yy}^{[\epsilon]} + O(De^2) + O(\epsilon^2), \\
\tau_{xy} &= \tau_{xy}^{[\ell]} + De\tau_{xy}^{[D]} + \epsilon\tau_{xy}^{[\epsilon]} + O(De^2) + O(\epsilon^2), \\
p &= p^{[\ell]} + Dep^{[D]} + \epsilon p^{[\epsilon]} + O(De^2) + O(\epsilon^2).
\end{aligned} \tag{25}$$

The leading term is the conventional lubrication solution denoted by superscript  $[\ell]$ . The two perturbation corrections are denoted by the superscripts  $[\epsilon]$  and  $[De]$ , respectively. Such a technique has been used in [2] for solving a torsional flow of a convected Jeffreys fluid between parallel disks. In the following sections, we illustrate the solution to the Maxwell equations for small  $De$  and  $\epsilon$  numbers

$$0 < De \ll \epsilon \ll 1.$$

In practice, for a typical journal bearing lubricated with a viscoelastic lubricant, it is found the relationship between  $De$  and  $\epsilon$  is  $De = O(\epsilon) \ll 1$  [10,27].

### 3.1. Zero-order solution

We substitute (25) in Eqs. (16)–(24) and obtain the leading order equations corresponding to the Newtonian case:

$$\begin{aligned}
\frac{\partial u^{[\ell]}}{\partial x} + \frac{\partial v^{[\ell]}}{\partial y} &= 0, \\
\tau_{xx}^{[\ell]} &= 0, \quad \tau_{yy}^{[\ell]} = -2 \frac{\partial v^{[\ell]}}{\partial y}, \\
\tau_{xy}^{[\ell]} &= -\frac{\partial u^{[\ell]}}{\partial y}, \quad \frac{\partial \tau_{xy}^{[\ell]}}{\partial y} + \frac{\partial p^{[\ell]}}{\partial x} = 0, \quad \frac{\partial p^{[\ell]}}{\partial y} = 0, \\
u^{[\ell]} &= 1, \quad v^{[\ell]} = 0, \quad \text{when } y = 0, \\
u^{[\ell]} = v^{[\ell]} &= 0, \quad \text{when } y = h(x), \\
p^{[\ell]} &= 0, \quad \text{when } x = 0, 1.
\end{aligned} \tag{26}$$

These equations can be easily solved in terms of the velocity and pressure yielding

$$u^{[\ell]} = \frac{h^2}{2} \frac{dp^{[\ell]}}{dx} \left( \frac{y^2}{h^2} - \frac{y}{h} \right) + 1 - \frac{y}{h}, \tag{27}$$

$$v^{[\ell]} = \frac{dh}{dx} \left( 2 - 3 \frac{h_m}{h} \right) \left( \frac{y^3}{h^3} - \frac{y^2}{h^2} \right), \tag{28}$$

$$\frac{dp^{[\ell]}}{dx} = 6 \frac{h - h_m}{h^3}, \tag{29}$$

where

$$h_m = \frac{\int_0^1 h^{-2}(x) dx}{\int_0^1 h^{-3}(x) dx}. \tag{30}$$

Integrating Eq. (29), we obtain the pressure distribution

$$p^{[\ell]}(x) = 6 \int_0^x h^{-2}(s) ds - 6h_m \int_0^x h^{-3}(s) ds. \tag{31}$$

Actually, this is a solution to the classical Reynolds' equation [3,5].

### 3.2. De-order solution

The  $De$ -order solution is now considered in this section. We first substitute (25) in (16)–(21), and then collect all order- $De$  terms to obtain the governing equations

$$\frac{\partial u^{[D]}}{\partial x} + \frac{\partial v^{[D]}}{\partial y} = 0, \tag{32}$$

$$\tau_{xx}^{[D]} = 2 \frac{\partial u^{[q]}}{\partial y} \tau_{xy}^{[q]} = -2 \left( \frac{\partial u^{[q]}}{\partial y} \right)^2, \quad (33)$$

$$\tau_{xy}^{[D]} + \frac{\partial u^{[D]}}{\partial y} = -u^{[q]} \frac{\partial \tau_{xy}^{[q]}}{\partial x} - v^{[q]} \frac{\partial \tau_{xy}^{[q]}}{\partial y} + \frac{\partial u^{[q]}}{\partial y} \tau_{yy}^{[q]}, \quad (34)$$

$$\tau_{yy}^{[D]} + 2 \frac{\partial v^{[D]}}{\partial y} = -u^{[q]} \frac{\partial \tau_{yy}^{[q]}}{\partial x} - v^{[q]} \frac{\partial \tau_{yy}^{[q]}}{\partial y} + 2 \frac{\partial v^{[q]}}{\partial y} \tau_{yy}^{[q]} + 2 \frac{\partial v^{[q]}}{\partial x} \tau_{xy}^{[q]}, \quad (35)$$

$$\frac{\partial \tau_{xx}^{[D]}}{\partial x} + \frac{\partial \tau_{xy}^{[D]}}{\partial y} + \frac{\partial p^{[D]}}{\partial x} = 0, \quad (36)$$

$$\frac{\partial p^{[D]}}{\partial y} = 0 \quad (37)$$

and the boundary conditions

$$u^{[D]} = v^{[D]} = 0, \quad \text{when } y = 0 \quad \text{and } y = h(x),$$

$$p^{[D]} = 0, \quad \text{when } x = 0, 1. \quad (38)$$

Note that the equation  $\tau_{xy}^{[q]} = -\frac{\partial u^{[q]}}{\partial y}$  has been used here to simplify Eq. (33). Similar expressions can be found in [18].

Substituting  $\tau_{xx}^{[D]}$  and  $\tau_{xy}^{[D]}$  from Eqs. (33) and (34) in Eq. (36), we obtain

$$-\frac{\partial^2 u^{[D]}}{\partial y^2} - 2 \frac{\partial}{\partial x} \left( \frac{\partial u^{[q]}}{\partial y} \right)^2 - \frac{\partial}{\partial y} \left( u^{[q]} \frac{\partial \tau_{xy}^{[q]}}{\partial x} \right) - \frac{\partial}{\partial y} \left( v^{[q]} \frac{\partial \tau_{xy}^{[q]}}{\partial y} \right) + \frac{\partial}{\partial y} \left( \tau_{yy}^{[q]} \frac{\partial u^{[q]}}{\partial y} \right) + \frac{\partial p^{[D]}}{\partial x} = 0. \quad (39)$$

From Eq. (37), we know that the viscoelastic pressure  $p^{[D]}$  is independent of  $y$ , hence,  $\partial^2 u^{[D]}/\partial y^2$  in Eq. (39) is also independent of  $y$ . We can integrate Eq. (39) twice with respect to  $y$  subject to the boundary condition (38), and we then obtain a general expression for the perturbation velocity

$$u^{[D]} = \frac{h^2}{2} \frac{dp^{[D]}}{dx} \left( \frac{y^2}{h^2} - \frac{y}{h} \right) + \frac{1}{h} \frac{dh}{dx} \left( 1 - 3 \frac{h_m}{h} \right) \left( 2 - 3 \frac{h_m}{h} \right) \left( \frac{y^2}{h^2} - \frac{y}{h} \right). \quad (40)$$

It should be noted that  $u^{[D]}$  is a quadratic function of  $y$  only, and the solution given by Tichy in [18] appears erroneous. A modified Reynolds' equation can be derived from the continuity equation

$$\frac{1}{12} \frac{d}{dx} \left( h^3 \frac{dp^{[D]}}{dx} \right) = \frac{d^2 h}{dx^2} \left( -\frac{1}{3} + \frac{3}{2} \frac{h_m}{h} - \frac{3}{2} \frac{h_m^2}{h^2} \right) + \frac{1}{h} \left( \frac{dh}{dx} \right)^2 \left( -\frac{3}{2} \frac{h_m}{h} + 3 \frac{h_m^2}{h^2} \right). \quad (41)$$

However, we must still find  $p^{[D]}$ . The best way to formulate an equation for the pressure  $p^{[D]}$  is to integrate the velocity  $u^{[D]}$  through the film from  $y = 0$  to  $y = h(x)$ , to obtain the net flow rate at order  $De$ . In fact, we have not yet used the continuity equation. We do so in an integral form to derive another constraint on the velocity field

$$h_d = \int_0^{h(x)} u^{[D]}(y) dy. \quad (42)$$

The constant  $h_d$  is not known at this point. Eq. (42) yields an equation for  $dp^{[D]}/dx$  as a function of  $h(x)$ ,  $dh/dx$ ,  $h_m$  and  $h_d$ ,

$$\frac{dp^{[D]}}{dx} = -18 \frac{h_m^2}{h^5} \frac{dh}{dx} + 18 \frac{h_m}{h^4} \frac{dh}{dx} - 4 \frac{1}{h^3} \frac{dh}{dx} - 12 \frac{h_d}{h^3}. \quad (43)$$

This is simply a first-order ordinary differential equation for the viscoelastic pressure gradient, which may be integrated to yield a solution  $p^{[D]}(x)$ . Since this solution satisfies a first-order equation, a constant of integration appears. A second unknown constant  $h_d$  appears in Eq. (43). Actually, these two constant can be uniquely defined if the boundary conditions (38) are imposed. Hence, we obtain an analytical solution for the pressure

$$p^{[D]}(x) = \frac{9}{2} \left( \frac{h_m^2}{h^4} - \frac{h_m^2}{h_0^4} \right) - 6 \left( \frac{h_m}{h^3} - \frac{h_m}{h_0^3} \right) + 2 \left( \frac{1}{h^2} - \frac{1}{h_0^2} \right) - 12 h_d \int_0^x \frac{1}{h^3(s)} ds \quad (44)$$

and

$$h_d = \left\{ \frac{3}{8} \left( \frac{h_m^2}{h_1^4} - \frac{h_m^2}{h_0^4} \right) - \frac{1}{2} \left( \frac{h_m}{h_1^3} - \frac{h_m}{h_0^3} \right) + \frac{1}{6} \left( \frac{1}{h_1^2} - \frac{1}{h_0^2} \right) \right\} \left( \int_0^1 \frac{1}{h^3(s)} ds \right)^{-1}, \quad (45)$$

where  $h_0$  and  $h_1$  are the values of  $h(x)$  at  $x = 0$  and  $x = 1$ , respectively.

### 3.3. $\epsilon$ -order solution

An  $\epsilon$ -order solution is considered in this section. We first substitute (25) into (16)–(24) and then collect all  $\epsilon$ -order terms to obtain the following governing equations

$$\frac{\partial u^{[\epsilon]}}{\partial x} + \frac{\partial v^{[\epsilon]}}{\partial y} = 0, \quad (46)$$

$$\tau_{xx}^{[\epsilon]} = -2 \frac{\partial u^{[\epsilon]}}{\partial x}, \quad \tau_{xy}^{[\epsilon]} + \frac{\partial u^{[\epsilon]}}{\partial y} = -\frac{\partial v^{[\epsilon]}}{\partial y}, \quad \tau_{yy}^{[\epsilon]} = -2 \frac{\partial v^{[\epsilon]}}{\partial y}, \quad (47)$$

$$\frac{\partial \tau_{xx}^{[\epsilon]}}{\partial x} + \frac{\partial \tau_{xy}^{[\epsilon]}}{\partial y} + \frac{\partial p^{[\epsilon]}}{\partial x} = 0, \quad (48)$$

$$\frac{\partial \tau_{xy}^{[\epsilon]}}{\partial x} + \frac{\partial \tau_{yy}^{[\epsilon]}}{\partial y} + \frac{\partial p^{[\epsilon]}}{\partial y} = 0, \quad (49)$$

with the boundary conditions

$$u^{[\epsilon]} = v^{[\epsilon]} = 0, \quad \text{when } y = 0 \quad \text{and} \quad y = h(x), \quad (50)$$

$$p^{[\epsilon]} - \frac{\partial v^{[\epsilon]}}{\partial y} = 0, \quad \text{when } x = 0 \quad \text{and} \quad x = 1. \quad (51)$$

Substituting  $\tau_{xy}^{[\epsilon]}$ ,  $\tau_{yy}^{[\epsilon]}$ ,  $\tau_{xx}^{[\epsilon]}$  and  $\tau_{xy}^{[\epsilon]}$  in Eqs. (48) and (49), the above equations can be simplified to

$$\frac{\partial p^{[\epsilon]}}{\partial x} = \frac{\partial^2 u^{[\epsilon]}}{\partial y^2} + 2 \frac{\partial^2 u^{[\epsilon]}}{\partial x^2} + \frac{\partial^2 v^{[\epsilon]}}{\partial y^2}, \quad (52)$$

$$\frac{\partial p^{[\epsilon]}}{\partial y} = \frac{\partial^2 v^{[\epsilon]}}{\partial y^2}, \quad (53)$$

where  $u^{[\epsilon]}$  and  $v^{[\epsilon]}$  are given in (27) and (28).

Following the procedure used in the previous section, we obtain a general expression for the velocity with the order- $\epsilon$  corrections

$$\begin{aligned} u^{[\epsilon]} = & \left( \frac{9h_m(h')^2}{h^5} - \frac{9(h')^2}{2h^4} - \frac{9h_m h''}{4h^4} + \frac{3h''}{2h^3} \right) y^4 + \left( \frac{3h_m h'}{h^4} - \frac{2h'}{h^3} - \frac{9h_m(h')^2}{h^4} + \frac{4(h')^2}{h^3} + \frac{3h_m h''}{h^3} - \frac{2h''}{h^2} \right) y^3 \\ & + \left( -\frac{6h_\epsilon}{h^3} - \frac{9h_m h'}{2h^3} + \frac{3h'}{h^2} - \frac{27h_m(h')^2}{10h^3} + \frac{21(h')^2}{10h^2} - \frac{9h_m h''}{20h^2} + \frac{3h''}{10h} \right) y^2 \\ & + \left( \frac{6h_\epsilon}{h^2} + \frac{3h_m h'}{2h^2} - \frac{h'}{h} + \frac{27h_m(h')^2}{10h^2} - \frac{8(h')^2}{5h} + \frac{h''}{5} - \frac{3h_m h''}{10h} \right) y, \end{aligned} \quad (54)$$

where  $h' = \frac{dh}{dx}$  and  $h'' = \frac{d^2h}{dx^2}$ .

After some algebraic manipulation, we obtain the pressure with the order- $\epsilon$  corrections

$$p^{[\epsilon]}(x, y) = \left( \frac{6h'}{h^3} - \frac{9h_m h'}{h^4} \right) y^2 + \left( \frac{6h_m h'}{h^3} - \frac{4h'}{h^2} \right) y - h_\epsilon \int_0^x \frac{12}{h^3(s)} ds + A_\epsilon(x) + B_\epsilon(x), \quad (55)$$

where  $h_\epsilon$ ,  $A_\epsilon$  and  $B_\epsilon$  are functions of  $x$  only. More detailed algebraic calculations are presented in Appendix A. Obviously, these solutions are cumbersome, but readily amenable to compute.

## 4. Numerical results and discussions

The asymptotic solution to the exact formulation of the UCM model given in (25) is the sum of the conventional lubrication solution, plus small corrections from the effects of the geometric parameter  $\epsilon$  and the viscoelastic property of fluid (the Deborah number  $De$ ). In physical terms, this condition is not restrictive because in the lubrication analysis the Deborah number  $De$  and the geometrical parameter  $\epsilon$  are always much less than unity [2,3,5,9,10].

To examine the influence of the film surface and the effect of the Deborah number, we investigate a viscoelastic thin film under the following contact dimensionless surface [18]

$$h(x) = \alpha + \beta x + \gamma(x^2 - x), \quad (56)$$

where  $\alpha$  is constant,  $\beta$  is the average curve slope and  $\gamma$  is the curvature. If  $\gamma$  is positive, the surface is concave, otherwise, the surface is convex. In Fig. 2, the surface slope is  $\beta = -0.5$ , and the curvatures are  $\gamma = -1$ ,  $\gamma = 0$  and  $\gamma = 1$ , respectively. The minimum film thickness for these surfaces shown in Fig. 2 is 0.5 and is attained at the fluid exit point  $x = 1$ . The surface defined by Eq. (56) is equivalent to one used by Tichy in [18] as  $\alpha = 0$ .

#### 4.1. Effect of viscoelasticity on the pressure

In this section, we examine the effect of the Deborah number  $De$  on the solution of (25). For simplicity, the dimensionless film surface (56) is used in this section with surface slopes  $\beta = -0.2$ ,  $\beta = -0.5$  and  $\beta = -0.8$ , and curvatures  $\gamma = -1.0$ ,  $\gamma = 0$  and  $\gamma = 1.0$ , respectively.

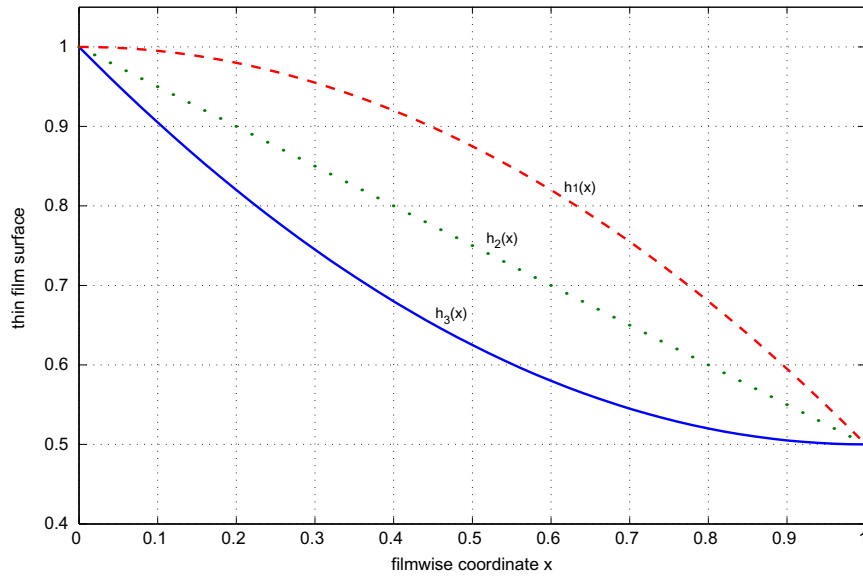


Fig. 2. Plots for three film surfaces:  $h_1(x) = 1 - 0.5x - 0.5(x^2 - x)$ ,  $h_2(x) = 1 - 0.5x$  and  $h_3(x) = 1 - 0.5x + 0.5(x^2 - x)$ , respectively.

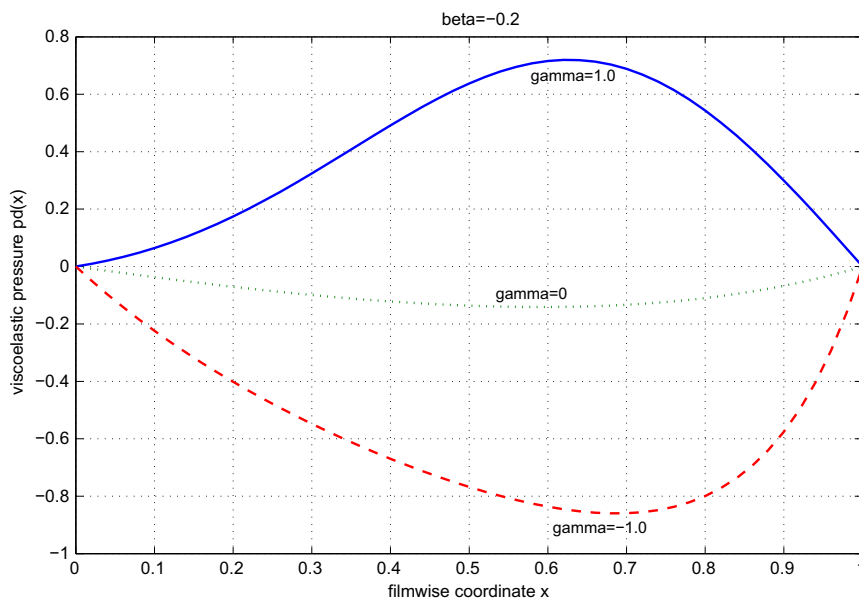


Fig. 3. Plots for viscoelastic pressure  $p^{Dl}(x)$  with an  $\alpha = 1$  and the slope  $\beta = -0.2$  and the curvatures  $\gamma = -1$ ,  $\gamma = 0$  and  $\gamma = 1$ , respectively.



Firstly, we examine the effect of a small value of the surface slope  $\beta = -0.2$  with curvatures  $\gamma = -1$ ,  $\gamma = 0$  and  $\gamma = 1$ , respectively. Fig. 3 shows plots of the viscoelastic pressures corresponding to these parameters. It is found that for a small surface slope,  $\beta = -0.2$ , the viscoelastic pressures are negative when  $\gamma = -1$  and  $\gamma = 0$ , and the maximum pressures,  $|p^{[D]}(x)|$ , are attained near the middle of the film. However, for the same surface slope, the viscoelastic pressure becomes positive when  $\gamma = 1$ , and the maximum pressure is attained near the middle of the film. Clearly, the positions of these three maximum pressures are not coincident, and surprisingly, they are not attained at the minimum film thickness point  $x = 1.0$ .

Secondly, we examine the effect of the mean value of the surface slope  $\beta = -0.5$  with different curvatures. The results are illustrated in Fig. 4, where the viscoelastic pressures  $p^{[D]}(x)$  are plotted with the curvature parameters  $\gamma = -1$ ,  $\gamma = 0$  and  $\gamma = 1$ , respectively. As expected, the viscoelastic pressures are negative when  $\gamma = -1$  and  $\gamma = 0$ . However, when  $\gamma = 1$ , the viscoelastic pressure becomes negative or positive, as shown in Fig. 4. This feature is not seen when the surface slope is small.

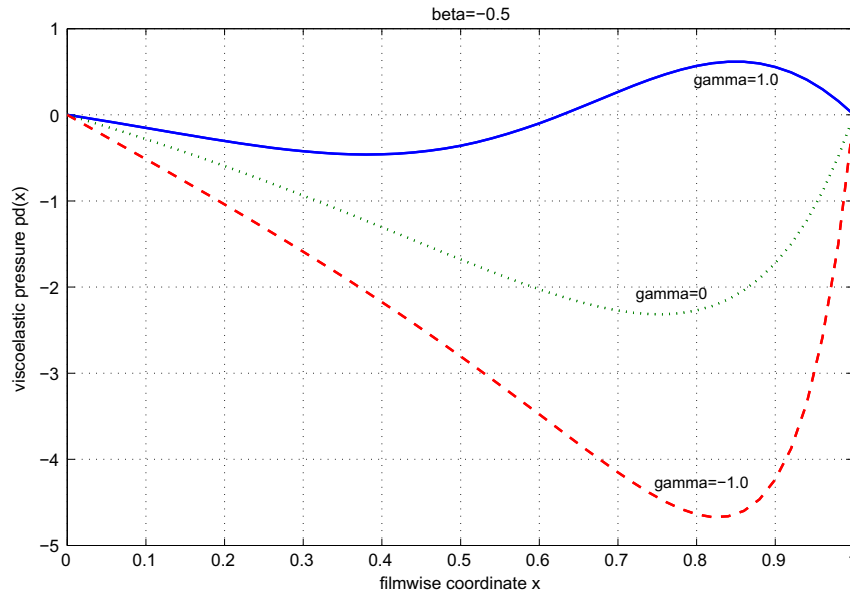


Fig. 4. Plots for viscoelastic pressure  $p^{[D]}$  with an  $\alpha = 1$  and the slope  $\beta = -0.5$  and the curvatures  $\gamma = -1$ ,  $\gamma = 0$  and  $\gamma = 1$ , respectively.

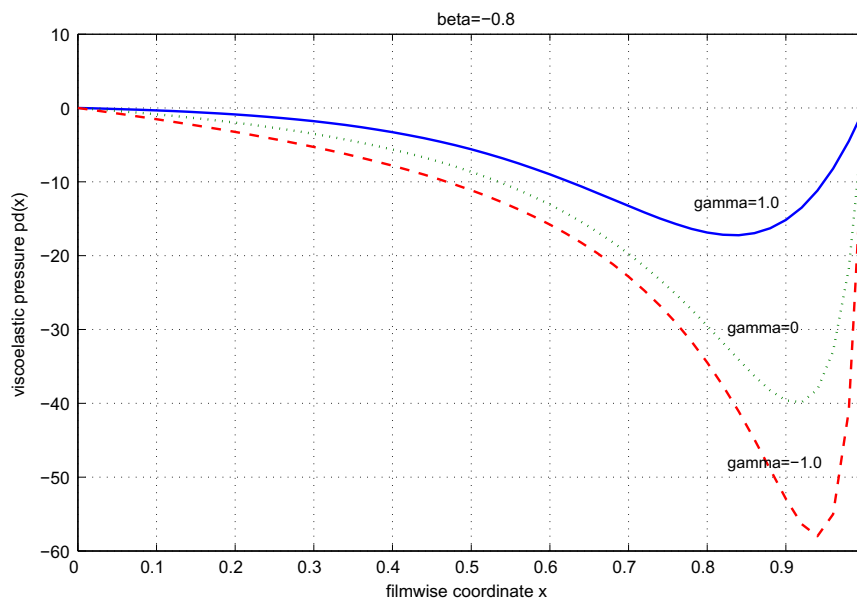
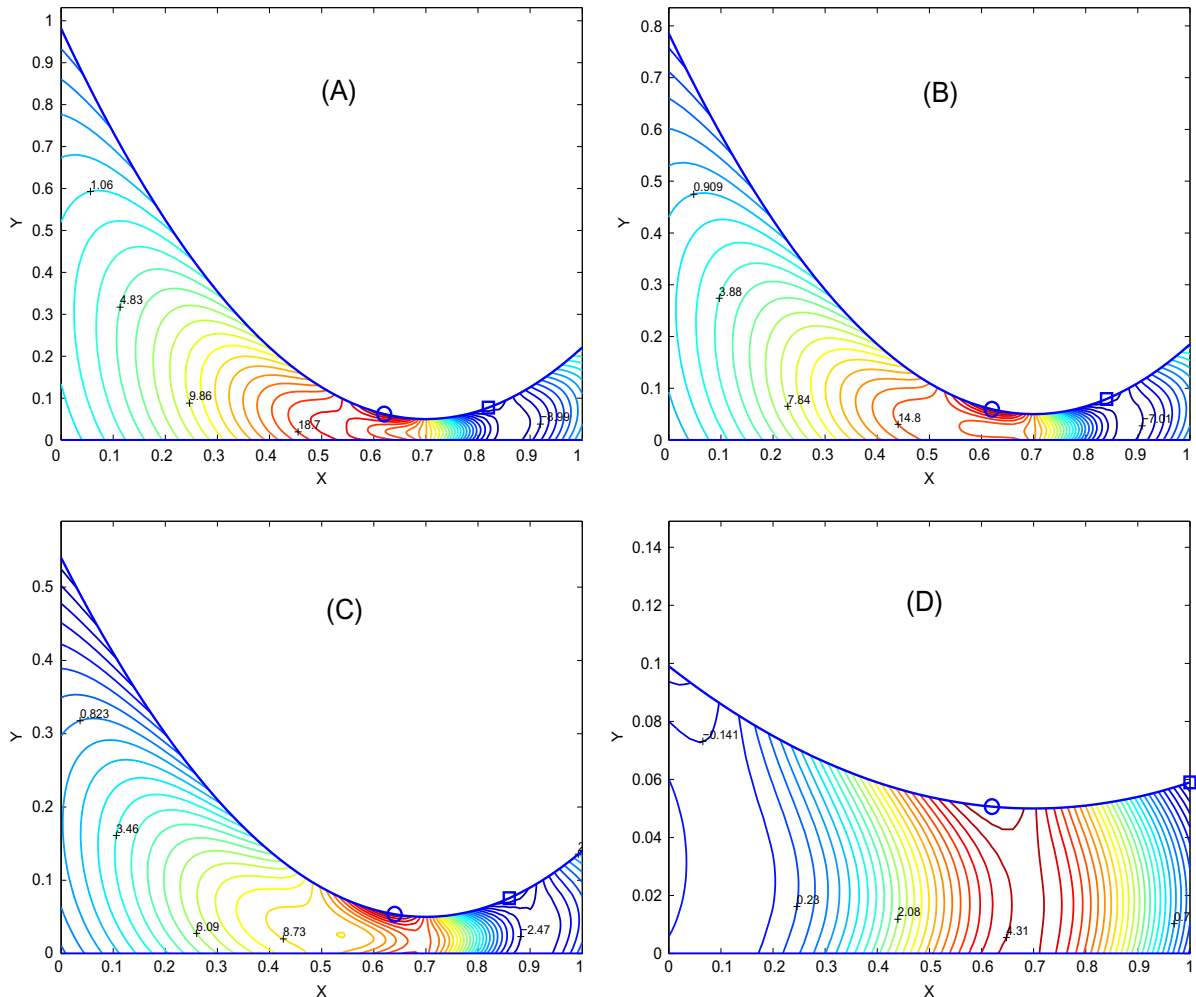


Fig. 5. Plot for viscoelastic pressure  $p^{[D]}$  with an  $\alpha = 1$  and the slope  $\beta = -0.8$  and the curvatures  $\gamma = -1$ ,  $\gamma = 0$  and  $\gamma = 1$ , respectively.

Furthermore, it is found that the maximum viscoelastic pressures,  $|p^{[D]}(x)|$ , are attained away from the middle of the film and approach to the fluid exit point, compared with the case of small surface slopes, as shown in Fig. 3.

Finally, we consider the effect of a large surface slope  $\beta = -0.8$  with different curvatures. Fig. 5 displays a comparison of the viscoelastic pressures for three curvatures. When the curvature changes from  $\gamma = 1$  to  $\gamma = -1$ , the absolute value of the viscoelastic pressure increases. This means that the viscoelastic effect on the pressure is much stronger when the average surface slope is bigger. The positions of the maximum pressures  $|p^{[D]}(x)|$  are very close to the fluid exit point. If we look more carefully at the sequences of Figs. 3–5, we find that the absolute values of the viscoelastic pressures increase with increasing the surface slope. For example, given a curvature, say,  $\gamma = -1$ , the maximum pressure  $|p^{[D]}(x)|$  is about 0.85 as  $\beta = -0.2$ , and about 4.5 as  $\beta = -0.5$ . However, when the surface slope is  $\beta = -0.8$ , the maximum pressure is dramatically increased over 55. Moreover, the positions of the maximum pressures move gradually from the point near the middle of the film to the point attained the minimum film thickness. We suspect that this occurs for the following reasons. When fluid enters the gap, material elements become more extended. As a consequence of this, and the viscoelasticity of the fluid, the first normal stress difference increases when the minimum film thickness point is approached. Thus, there will be a gradient in the first normal stress difference: it is highest near the minimum film thickness point and decreases upstream. These higher tensions near the point of the minimum film thickness will tend to pull fluid toward the minimum point. Because more fluid will be entering the gap, the maximum pressure may increase to turn back some of the additional fluid.

In general, the viscoelastic pressure may either increase or decrease depending on combinations of the surface slope and its curvature. The larger the surface slope, the stronger the effect of the viscoelastic pressure. Numerical results demonstrate that the viscoelasticity plays an important role in determining the pressure distributions, and it should be taken into account in the analysis of the thin film flows.



**Fig. 6.** The pressure perturbation solution  $p^{[e]}(x, y)$  with the film surface  $h(x) = \alpha + \beta(x - \gamma)^2$ , where  $\alpha = 0.05$ ,  $\gamma = 0.7$  and (A)  $\beta = 1.9$ , (B)  $\beta = 1.5$ , (C)  $\beta = 1.0$  and (D)  $\beta = 0.1$ , respectively. ○ is denoted the maximum pressure point and □ is the minimum pressure point.

#### 4.2. Effect of $\epsilon$ on the pressure

In this section we investigate the effect of  $\epsilon$  on the pressure field. The dimensionless film surface is defined as

$$h(x) = \alpha + \beta(x - \gamma)^2, \quad (57)$$

where  $\alpha$  is the minimum film thickness attained at  $x = \gamma$ .

We first examine the effect of the surface curvature on the solution of the pressure  $p^{[\epsilon]}$ . Fig. 6 shows the pressure contours with the surface curvatures varying from  $\beta = 0.1$  to  $\beta = 1.9$ . As expected, the maximum pressure  $p^{[\epsilon]}$  decreases with reducing the surface curvature. For example, when  $\beta = 1.9$  the maximum pressure is  $p^{[\epsilon]} = 24.19$ , and  $\beta = 1.0$ , the maximum pressure is 15.31. Similarly, when  $\beta = 0.1$  the maximum pressure reduces to 4.681. We suspect that this behaviour is caused by the surface curvature as the flow anticipates the converging area. The more abrupt the surface curvature, the more effect on the pressure increasing. Furthermore, we found that the pressure reaches to a maximum point on the surface just at the upstream of the minimum film thickness point, and decreases with increasing flow area, then gradually reaches a minimum point at somewhere before the fluid exits. The exact locations of the maximum and the minimum pressure points are shown in Fig. 6 marked by  $\circ$  and  $\square$ , respectively.

In order to quantify the effect of  $\epsilon$  on the pressure  $p^{[\epsilon]}$ , more calculations are carried out for different minimum film thicknesses. To do this, we need to take the parameters  $\beta$  and  $\gamma$  to be fixed and vary the  $\alpha$  only. Fig. 7 shows the surface having the same curvature  $\beta = 1.0$ , with different minimum film thicknesses,  $\alpha = 0.01, 0.05, 0.1$  and  $0.5$ , respectively. As expected, increasing the minimum film thickness results in decreasing the pressure  $p^{[\epsilon]}$ . For example, we found that the maximum pressure  $p^{[\epsilon]}$  is 35.49 when  $\alpha = 0.01$ , and 15.31 when  $\alpha = 0.05$ . If  $\alpha$  further increases from 0.1 to 0.5, the maximum pressure

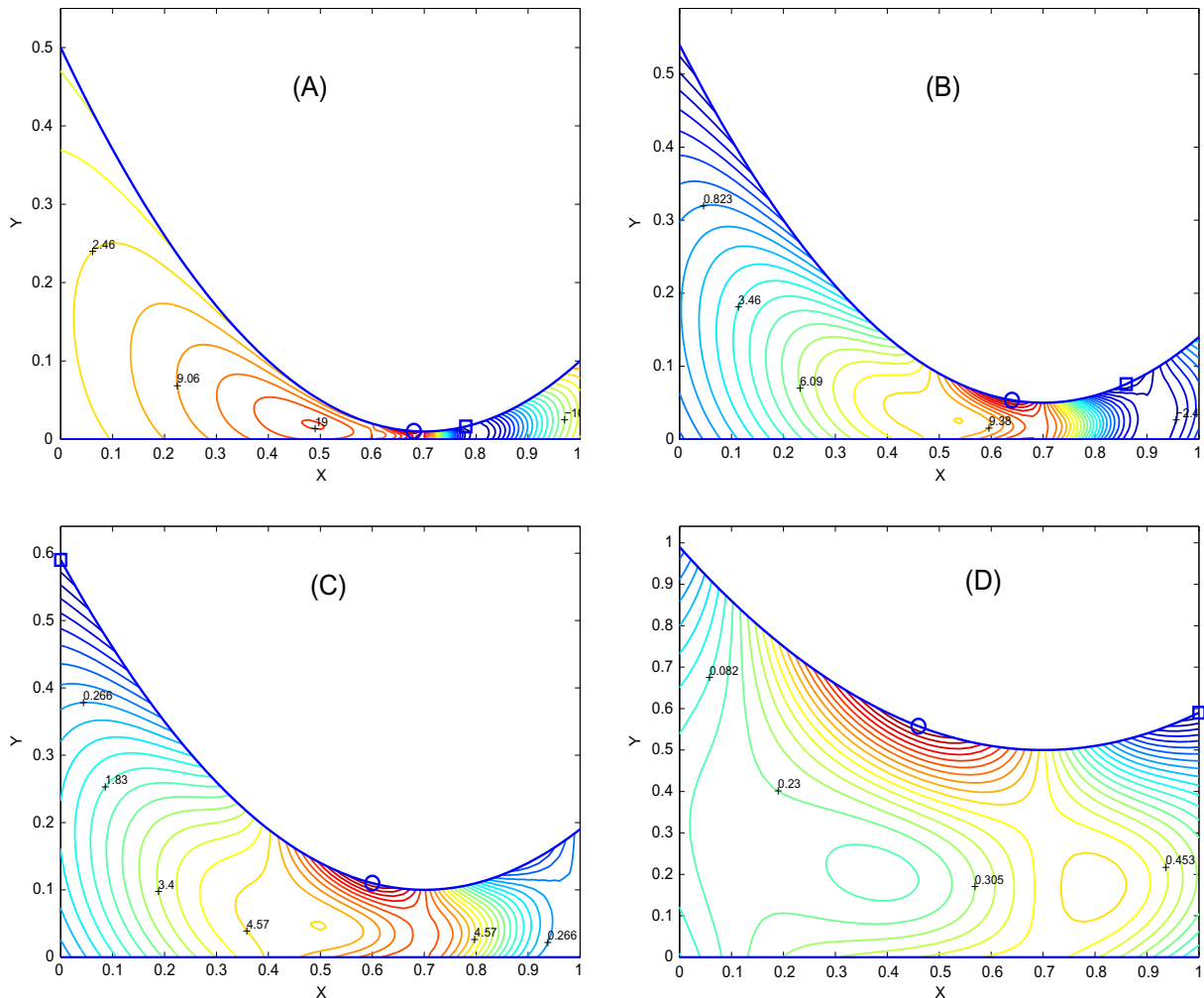


**Fig. 7.** A comparison of the pressure contour plots for  $p^{[\epsilon]}(x, y)$  with the film surfaces  $h(x) = \alpha + \beta(x - \gamma)^2$ , when  $\beta = 1.0$ ,  $\gamma = 0.7$  and (A)  $\alpha = 0.01$ , (B)  $\alpha = 0.05$ , (C)  $\alpha = 0.1$  and (D)  $\alpha = 0.5$ , respectively.  $\circ$  is denoted the maximum pressure point and  $\square$  is the minimum pressure point.

decreases from 8.48 to 1.34. The positions of the maximum and minimum pressures are shown in Fig. 7 marked by  $\circ$  and  $\square$ , respectively.

#### 4.3. Effect of the minimum film thickness on the pressure

As discussed in the previous sections, the influence of the film surface shape is of considerable importance in the thin film analysis. In order to further examine such a influence on the pressure distribution, we consider three different film surfaces in this section:  $h_1(x) = 0.59 - 0.4x + (x^2 - x)$ ,  $h_2(x) = 0.565 - 0.4x + (x^2 - x)$ , and  $h_3(x) = 0.54 - 0.4x + (x^2 - x)$ , plotted in Fig. 8. Unlike the surfaces given in Fig. 2, these surfaces have the same average slope and curvature parameters, but, different minimum film thicknesses attained at the same point  $x = 0.7$ , as shown in Fig. 8. In these three surfaces, the minimum film thicknesses are  $h_1^{\min} = 0.1$ ,  $h_2^{\min} = 0.075$  and  $h_3^{\min} = 0.05$ , respectively. A comparison of the viscoelastic pressures corresponding to these three surfaces are illustrated in Fig. 9, where it can be seen that all maximum pressures are located almost at the same point,  $x = 0.7$ , which is the position of the minimum film thickness for all three cases. More important, we found that the magnitude of the viscoelastic pressure increases dramatically with decreasing the minimum film thickness. Actually, we

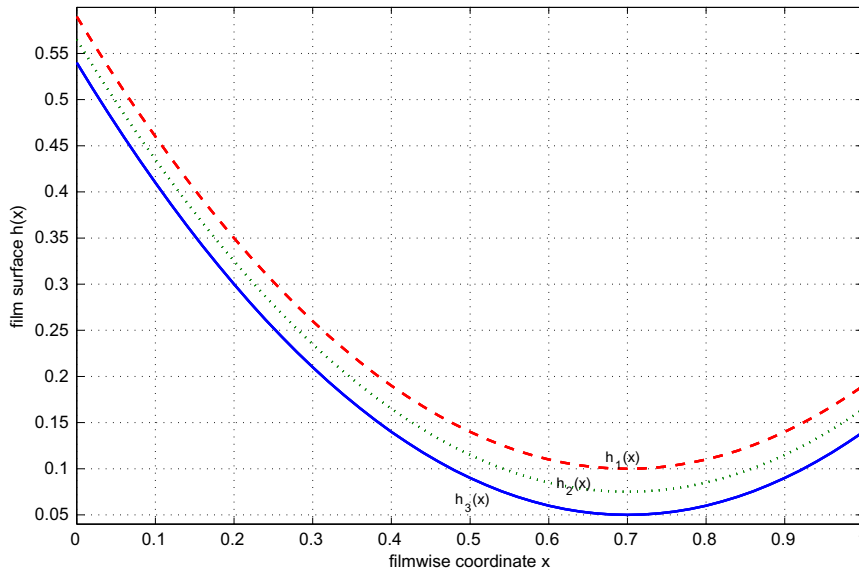


Fig. 8. Three different surfaces:  $h_1(x) = 0.59 - 0.4x + (x^2 - x)$ ,  $h_2(x) = 0.565 - 0.4x + (x^2 - x)$ , and  $h_3(x) = 0.54 - 0.4x + (x^2 - x)$ .

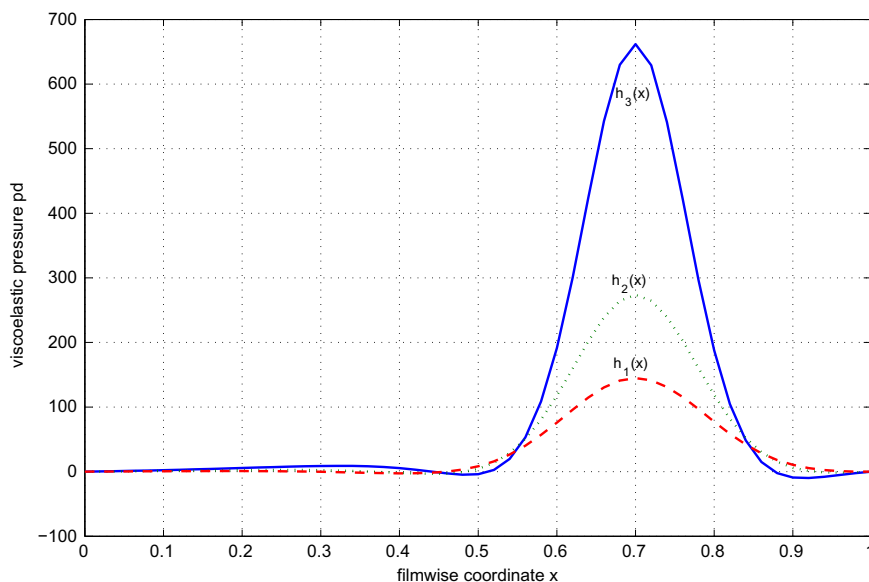


Fig. 9. The viscoelastic pressure plots corresponding to the three different surfaces  $h_1(x)$ ,  $h_2(x)$  and  $h_3(x)$  given in Fig. 8.

found that, when the minimum film thickness is  $h_1^{\min} = 0.1$ , the maximum pressure is 144.83 for the surface  $h_1(x)$ ; when it is  $h_2^{\min} = 0.075$ , the maximum pressure increases to 273.61. Moreover, when the film thickness decreases to  $h_3^{\min} = 0.05$ , the maximum pressure rapidly increases to 661.81. This finding clearly suggests that there is a significant pressure enhancement when the minimum film thickness becomes small. Such a phenomenon is not observed in Newtonian fluids. It is worth pointing out that this viscoelastic pressure enhancement has been observed in experimental measurements for a journal bearing system [7,8], where it was found that the viscoelasticity does indeed produce a measurable effect on lubrication characteristics at the higher eccentricity ratios (equivalent to the smaller minimum film thicknesses). Thus, it seems reasonable that our numerical predictions here are in good agreement with the experimental observations [7,8] in regard to the viscoelastic pressure enhancement in the thin film flows.

It should be remarked that although the minimum film thickness is an important criterion for the correction of the pressure  $p^{[\epsilon]}$  as shown in the previous section, it does not have a profound effect on the total pressure  $p$  compared with the effect of the viscoelastic pressure  $p^{[D]}$ . Great insight can be obtained if Fig. 7(B) is viewed along with surface  $h_3$  in Fig. 9, where the surfaces are exactly the same. Comparing these two figures, we found that the maximum pressures are significantly different in terms of the magnitudes. For instance, the maximum pressure  $p^{[D]}$  is over 600, but, the maximum pressure  $p^{[\epsilon]}$  is only 15. This behaviour clearly shows that the total pressure  $p$  is dominated by the viscoelastic pressure  $p^{[D]}$ , but not the  $p^{[\epsilon]}$ . Thus, the pressure correction  $p^{[\epsilon]}$  can be ignored in the asymptotic solution of (25), when the minimum film thickness is sufficiently small. Furthermore, from numerical calculations we might conclude that, both corrections  $p^{[D]}$  and  $p^{[\epsilon]}$  can be neglected in the asymptotic solution (25), when the minimum film thickness is large enough, say, for example,  $h_{\min} > 0.5$ . However, care must be taken when the minimum film thickness is sufficiently small, say,  $h_{\min} < 0.5$ , since in this situation the pressures  $p^{[D]}$  and  $p^{[\epsilon]}$  are no longer small, and they increase significantly with decreasing the minimum film thickness. However, the viscoelastic pressure  $p^{[D]}$  plays a dominated role in the total pressure distribution when the film thickness is sufficiently small.

## 5. Conclusions

In this paper, we have readdressed the question as to whether the viscoelastic properties of a viscoelastic lubricant can have an effect on lubrication performance characteristics in thin film flows. A perturbation analysis based on the upper convected Maxwell constitutive equation was presented by employing characteristic lubricant relaxation times in an order of magnitude analysis. Despite inherent limitations of the perturbation method, the approach presented here demonstrates a reasonable way to determine the viscoelastic effects on the lubrication performance characteristics. The calculations in this paper are based on a UCM fluid model with constant viscosity and relaxation time. Numerical simulations indicate that there is a significant enhancement on the viscoelastic pressure when the minimum film thickness is sufficiently small. This mechanism is associated with a beneficial effect of viscoelasticity on lubrication characteristics as observed in experimental measurements [7,8]. Furthermore, we found that the total pressure  $p$  is dominated by the viscoelastic pressure  $p^{[D]}$ , when the minimum film thickness is small, but not the  $p^{[\epsilon]}$ . Evidence is emerging that the normal stress difference is a stronger function of the pressure than the shear stress [7]. If this is the case, it is not surprising that the beneficial effects of viscoelasticity show up in the experiments [8] and numerical simulations presented here when the minimum film thickness is small, the pressures are likely to be high enough for the normal stress amplification effect to be relevant. If this is a correct diagnosis, there is clearly a need for a detailed study of the pressure dependence of the rheometrical properties of lubricants [7]. In this respect, the availability of the current study can be viewed as an important development. However, an assumption of the thin film surface,  $h(x)$ , is a limitation of the present study, since, in reality, the surface function  $h(x)$  depends not only on the spatial but also on the temporal. In conclusion, we have addressed and assessed some of the issues concerning viscoelastic effects on lubricant in the thin film flows, although further work is needed to extend the current method to other fluid models and flow configurations.

## Acknowledgements

The authors are indebted for many discussions with colleagues in the Faculty of Technology, De Montfort University. XKL and LYS are partially supported by an open project (09RM01) by the Centre South University of Forestry and Technology, China. RZ is supported by the grant from Southern Yangtze University, China.

## Appendix A

A full detail of the derivations of  $p^{[\epsilon]}$  and  $u^{[\epsilon]}$  is given in this appendix.

We first substitute  $\tau_{xy}^{[\epsilon]}$ ,  $\tau_{yy}^{[\epsilon]}$ ,  $\tau_{xx}^{[\epsilon]}$  and  $\tau_{xy}^{[\epsilon]}$  in Eqs. (48) and (49) and obtain

$$\frac{\partial p^{[\epsilon]}}{\partial x} = \frac{\partial^2 u^{[\epsilon]}}{\partial x^2} + 2 \frac{\partial^2 u^{[\epsilon]}}{\partial x^2} + \frac{\partial^2 v^{[\epsilon]}}{\partial y^2}, \quad (58)$$

$$\frac{\partial p^{[\epsilon]}}{\partial y} = \frac{\partial^2 v^{[\epsilon]}}{\partial y^2}, \quad (59)$$

where  $u^{[\epsilon]}$  and  $v^{[\epsilon]}$  are given in (27) and (28).

From Eq. (59), we have

$$\frac{\partial}{\partial y} \left( p^{[\epsilon]}(x, y) - \frac{\partial v^{[\epsilon]}}{\partial y} \right) = 0. \quad (60)$$

This means

$$p^{[\epsilon]}(x, y) - \frac{\partial v^{[\epsilon]}}{\partial y} = g(x), \quad (61)$$

where  $g(x)$  is a unknown function with respect to  $x$  only. Thus, the pressure  $p^{[\epsilon]}(x)$  is

$$p^{[\epsilon]}(x, y) = g(x) + \frac{\partial v^{[\epsilon]}}{\partial y} = g(x) - \frac{\partial u^{[\epsilon]}}{\partial x}. \quad (62)$$

Now we differentiate Eq. (62) with respect to  $x$  and substitute it in Eq. (58) to eliminate the pressure gradient, and then we obtain

$$\frac{\partial^2 u^{[\epsilon]}}{\partial y^2} = \frac{dg}{dx} - 3 \frac{\partial^2 u^{[\epsilon]}}{\partial x^2} - \frac{\partial^2 v^{[\epsilon]}}{\partial y^2}. \quad (63)$$

Moreover, we rewrite the above equation in the form

$$\begin{aligned} \frac{\partial^2 u^{[\epsilon]}}{\partial y^2} = & \left( \left( \frac{108h_m}{h^5} - \frac{54}{h^4} \right) (h')^2 + \left( \frac{18}{h^3} - \frac{27h_m}{h^4} \right) h'' \right) y^2 \\ & + \left( \left( \frac{18h_m}{h^4} - \frac{12}{h^3} \right) h' + \left( \frac{24}{h^3} - \frac{54h_m}{h^4} \right) (h')^2 + \left( \frac{18h_m}{h^3} - \frac{12}{h^2} \right) h'' \right) y + \left( \frac{4}{h^2} - \frac{6h_m}{h^3} \right) h' + \frac{dg}{dx}. \end{aligned} \quad (64)$$

Integrating the above twice formally with respect to  $y$ , we obtain the velocity with  $\epsilon$ -order corrections

$$\begin{aligned} u^{[\epsilon]} = & \frac{1}{2} \frac{dg}{dx} y^2 - \frac{h}{2} \frac{dg}{dx} y + \left( \left( \frac{3h_m}{h^4} - \frac{2}{h^3} \right) y^3 + \left( \frac{2}{h^2} - \frac{3h_m}{h^3} \right) y^2 \right) h' + \left( \left( \frac{9h_m}{h^5} - \frac{9}{2h^4} \right) y^4 + \left( \frac{4}{h^3} - \frac{9h_m}{h^4} \right) y^3 + \frac{1}{2h} y \right) (h')^2 \\ & + \left( \left( \frac{3}{2h^3} - \frac{9h_m}{4h^4} \right) y^4 + \left( \frac{3h_m}{h^3} - \frac{2}{h^2} \right) y^3 + \left( \frac{1}{2} - \frac{3h_m}{4h} \right) y \right) h''. \end{aligned} \quad (65)$$

At this stage the velocity profile is explicit in terms of  $y$  and an unknown gradient function  $g(x)$ . Hence, we now must find  $g(x)$ . In order to do this, we integrate the velocity  $u^{[\epsilon]}$  across the film from  $y = 0$  to  $y = h(x)$  and obtain the net flow rate  $h_\epsilon$  at order of  $\epsilon$

$$h_\epsilon = \int_0^{h(x)} u^{[\epsilon]}(y) dy. \quad (66)$$

From this we find

$$\frac{dg}{dx} = -\frac{12h_\epsilon}{h^3} - \frac{3h_m}{h^3} h' + \frac{2}{h^2} h' - \frac{27h_m}{5h^3} (h')^2 + \frac{21}{5h^2} (h')^2 - \frac{9h_m}{10h^2} h'' + \frac{3}{5h} h''. \quad (67)$$

This is simply a first-order ordinary differential equation for  $g(x)$ , which can be integrated to yield a solution

$$g(x) = g_0 - \int_0^x \frac{12h_\epsilon}{h^3(s)} ds + A_\epsilon(x) + B_\epsilon(x), \quad (68)$$

where  $A_\epsilon(x)$  and  $B_\epsilon(x)$  are defined as

$$A_\epsilon(x) = \frac{3h_m}{2} \left( \frac{1}{h^2(x)} - \frac{1}{h_0^2} \right) - 2 \left( \frac{1}{h(x)} - \frac{1}{h_0} \right) \quad (69)$$

and

$$B_\epsilon(x) = \int_0^x \left\{ \left( \frac{21}{5h^2(s)} - \frac{27h_m}{5h^3(s)} \right) (h'(s))^2 + \left( \frac{3}{5h(s)} - \frac{9h_m}{10h^2(s)} \right) h''(s) \right\} ds, \quad (70)$$

where  $h_0$  is the value of  $h(x)$  at  $x = 0$ .

Finally, we need to find the values of two constants  $g_0$  and  $h_\epsilon$ , which are calculated straightforward from the pressure boundary condition (51)

$$g_0 = 0 \quad (71)$$

and

$$h_\epsilon = \frac{1}{12} (A_\epsilon(1) + B_\epsilon(1)) \left( \int_0^1 \frac{1}{h^3(s)} ds \right)^{-1}, \quad (72)$$

where  $A_\epsilon(1)$  and  $B_\epsilon(1)$  are the values of  $A_\epsilon(x)$  and  $B_\epsilon(x)$  at  $x = 1$ , respectively.

There has been a tedious algebraic calculation, but it has let to an explicit expression for the pressure

$$p^{[e]}(x, y) = \left( \frac{6h'}{h^3} - \frac{9h_m h'}{h^4} \right) y^2 + \left( \frac{6h_m h'}{h^3} - \frac{4h'}{h^2} \right) y - h_\epsilon g \int_0^x \frac{12}{h^3(s)} ds + A_\epsilon(x) + B_\epsilon(x). \quad (73)$$

## References

- [1] H.A. Barnes, J.F. Hutton, K. Walters, *An Introduction to Rheology*, Elsevier, Amsterdam, 1989.
- [2] R.B. Bird, R.C. Armstrong, O. Hassager, *Dynamics of Polymeric Liquids: Fluid Mechanics*, Wiley, New York, 1987.
- [3] A. Cameron, *Basic Lubrication Theory*, Ellis Horwood, Chichester, 1981.
- [4] O. Pinkus, B. Sternlicht, *Theory of Hydrodynamic Lubrication*, McGraw-Hill, New York, 1961.
- [5] R.I. Tanner, *Engineering Rheology*, second ed., Oxford University Press, Oxford, 2000.
- [6] G.W. Roberts, K. Walters, Oil viscoelastic effects in journal bearing lubrication, *Rheol. Acta* 31 (1992) 55.
- [7] B.P. Williamson, K. Walters, T.B. Bates, R.C. Coy, A.L. Milton, The viscoelastic properties of multigrade oils and their effect on journal-bearing characteristics, *J. Non-Newtonian Fluid Mech.* 73 (1997) 115.
- [8] T.W. Bates, B.P. Williamson, J.A. Spearot, C.K. Murphy, A correlation between engine oil rheology and oil film thickness in engine journal bearing, *Soc. Automotive Eng., Paper No. 860376*, 1986.
- [9] J.M. Crochet, K. Walters, Computational rheology: a new science, *Endeavour, New Ser.* 17 (1993) 64.
- [10] A.Z. Szeri, *Fluid Film Lubrication Theory and Design*, Cambridge University Press, 1998.
- [11] A. Berker, M.G. Bouldin, S.J. Kleiss, W.E. van Arsdale, Effect of polymer flow in journal bearings, *J. Non-Newtonian Fluid Mech.* 56 (1995) 333.
- [12] A. Rastogi, R.K. Gupta, Lubricant elasticity and the performance of dynamically loaded journal bearings, *J. Rheol.* 34 (1990) 1337.
- [13] A.Z. Szeri, Some extensions of the lubrication theory of Osborne Reynolds, *ASME J. Tribol.* 109 (1987) 21.
- [14] M.J. Davies, K. Walters, The behaviour of non-Newtonian lubricants in journal bearings – a theoretical study, in: *Rheology of Lubricants*, Applied Science Publishers, 1972, p. 16.
- [15] A.R. Davies, X.K. Li, Numerical modelling of pressure and temperature effects in viscoelastic flow between eccentrically rotating cylinders, *J. Non-Newtonian Fluid Mech.* 54 (1994) 331.
- [16] J. Engmann, C. Servais, B. Burbidge, Squeeze flow theory and application to rheometry: a review, *J. Non-Newtonian Fluid Mech.* 132 (2005) 1.
- [17] E.R. Khayat, Transient two-dimensional coating flow of a viscoelastic fluid on a substrate of arbitrary shape, *J. Non-Newtonian Fluid Mech.* 95 (2000) 199.
- [18] J.A. Tichy, Non-Newtonian lubrication with the convected Maxwell model, *Trans. ASME* 118 (1996) 344.
- [19] Y. Zhang, K. Matar, R. Craster, Surfactant spreading on a thin weakly viscoelastic film, *J. Non-Newtonian Fluid Mech.* 105 (2002) 53.
- [20] R. Zhang, X.K. Li, Non-Newtonian effects on lubricant thin film flows, *J. Eng. Math.* 51 (2004) 1.
- [21] R. Zhang, X. He, S. Yang, X.K. Li, Perturbation solution of non-Newtonian lubrication with the convected Maxwell model, *ASME J. Tribol.* 127 (2005) 302.
- [22] X.K. Li, D. Gwynnlyw, A.R. Davies, T.N. Phillips, Three-dimensional effects in dynamically loaded journal bearings, *Int. J. Numer. Meth. Fluids* 29 (1999) 311.
- [23] S. Middleman, *Modelling Axisymmetric Flows*, Academic Press, 1995.
- [24] D. Dowson, G.R. Higginson, *Elastic-hydrodynamic Lubrication*, Pergamon Press, 1997.
- [25] D. Dowson, C.M. Taylor, Cavitation in bearings, *Annu. Rev. Fluid Mech.* 11 (1979) 35.
- [26] C.E. Brennen, *Cavitation and Bubble Dynamics*, Oxford University Press, Oxford, 1995.
- [27] D. Bourgin, Fluid-film flows of differential fluids of complexity  $n$  dimensional approach-applications to lubrication theory, *ASME J. Lubr. Technol.* 101 (1979) 140.